

# Vibronic coupling in $C_{60}^-$ anion revisited: Precise derivations from photoelectron spectra and DFT calculations

Naoya Iwahara,<sup>1</sup> Tohru Sato,<sup>1,2,\*</sup> Kazuyoshi Tanaka,<sup>1</sup> and Liviu F. Chibotaru<sup>3,†</sup>

<sup>1</sup>*Department of Molecular Engineering, Graduate School of Engineering, Kyoto University, Kyoto 615-8510, Japan*

<sup>2</sup>*Fukui Institute for Fundamental Chemistry, Kyoto University,  
Takano-Nishihiraki-cho 34-4, Sakyo-ku, Kyoto 606-8103, Japan*

<sup>3</sup>*Division of Quantum and Physical Chemistry, University of Leuven, Celestijnenlaan 200F, B-3001 Leuven, Belgium*

The vibronic coupling constants of  $C_{60}^-$  are derived from the photoelectron spectrum measured by Wang *et al.* [X. B. Wang, H. K. Woo, and L. S. Wang, *J. Chem. Phys.*, **123**, 051106 (2005).] at low temperature with high-resolutions. We find that the couplings of the Jahn–Teller modes of  $C_{60}^-$  are weaker than the couplings reported by Gunnarsson *et al.* [O. Gunnarsson, H. Handschuh, P. S. Bechthold, B. Kessler, G. Ganteför, and W. Eberhardt, *Phys. Rev. Lett.*, **74**, 1875 (1995)]. The total stabilization energy after  $h_g$  and  $a_g$  modes is reduced with respect to the previous derivation of Gunnarsson *et al.* by 30 %. The computed vibronic coupling constants using DFT with B3LYP functional agree well with the new experimental constants, so the discrepancy between theory and experiment persistent in the previous studies is basically solved.

## I. INTRODUCTION

Much attention has been paid to the Jahn–Teller effect of fullerene ( $C_{60}$ ) in various electronic states not only because the Jahn–Teller effect is an interesting problem in molecular physics<sup>1</sup> but also because it is expected to play an important role in the mechanism of the superconductivity in alkali-doped fullerenes.<sup>2</sup> Thus, the strength of the electron-vibration coupling (vibronic coupling) of  $C_{60}$  which characterizes the Jahn–Teller effect has been one of the important topics. The vibronic coupling constants (VCCs) have been estimated experimentally<sup>3–5</sup> and theoretically<sup>6–14</sup>.

In the experimental studies of vibronic coupling in fullerene, a landmark is the photoelectron spectroscopy (PES) of  $C_{60}^-$  in gas phase by Gunnarsson *et al.*<sup>3</sup> As  $C_{60}^-$  is one of the most studied systems, in addition to this experimental work, computational works have been performed by many authors. However, discrepancy between the coupling constants of the experimental and theoretical works have been reported.<sup>3,11,12</sup> The theoretical stabilization energies as estimated by density functional theory (DFT) calculation were always obtained smaller than that derived from the experiment of Gunnarsson *et al.* Besides uncertainties intrinsic to the DFT method, whose predictions depend on the used exchange-correlation functional, one should note that the derivation of vibronic coupling constants in Ref. 3 is not perfect either. First, the thermal excitations were not included in the simulation, although the vibrational temperature of  $C_{60}^-$  was estimated about 200 K in the experiment. Second, not all vibronic coupling constants have been estimated from the spectrum because of the low resolution. For the same reason, the computed VCCs of totally symmetric modes were used to simulate the PES.

Recently, Wang *et al.* remeasured photoelectron spectra of  $C_{60}^-$ .<sup>15</sup> In their experiment, the vibrational temperature of  $C_{60}^-$  is between 70 K and 90 K and the resolution is about 16 meV, i.e., much smaller than the resolution of

40 meV in the experiment of Gunnarsson *et al.* Accordingly, the spectrum of Wang *et al.* is narrower and has more structures, therefore, it is expected to yield more reliable coupling constants.

In this work, we simulate the photoelectron spectra of Wang *et al.*<sup>15</sup> and Gunnarsson *et al.*<sup>3</sup> and give new derivations of the VCCs of  $C_{60}^-$ . We also compute the VCCs of  $C_{60}^-$  using the DFT method and compare them with the experimental values.

## II. THE SOLUTION OF THE JAHN–TELLER PROBLEM OF $C_{60}^-$

The equilibrium geometry of neutral fullerene is taken as the reference nuclear configuration. At this reference structure, the ground electronic state of  $C_{60}^-$  is  $T_{1u}$ . According to the selection rule, the  $T_{1u}$  electronic state couples with two  $a_g$  and eight  $h_g$  vibrational modes:

$$[T_{1u}^2] = a_g \oplus h_g. \quad (1)$$

We consider the linear  $T_{1u} \otimes (2a_g \oplus 8h_g)$  Jahn–Teller Hamiltonian. The Hamiltonian is written as follows:

$$H = \sum_{i=1}^2 \left[ \frac{1}{2} \left( P_{a_g(i)}^2 + \omega_{a_g(i)}^2 Q_{a_g(i)}^2 + V_{a_g(i)} Q_{a_g(i)} \right) \right] \hat{I} \\ + \sum_{\mu=1}^8 \sum_{m=-2}^2 \left[ \frac{1}{2} \left( P_{h_g(\mu)m}^2 + \omega_{h_g(\mu)}^2 Q_{h_g(\mu)m}^2 \right) \hat{I} \right. \\ \left. + \sqrt{\frac{5}{2}} (-1)^m V_{h_g(\mu)} Q_{h_g(\mu)m} \hat{C}_{-m} \right], \quad (2)$$

where  $Q_{\Gamma(\mu)m}$  is the mass-weighted normal coordinate of  $m$  element of the  $\Gamma(\mu)$  mode ( $\Gamma = a_g, h_g$ ),  $P_{\Gamma(\mu)m}$  is the conjugate momentum of the normal coordinate  $Q_{\Gamma(\mu)m}$ ,  $\omega_{\Gamma(\mu)}$  is the frequency of the  $\Gamma(\mu)$  mode,  $V_{\Gamma(\mu)}$  is the VCC of the  $\Gamma(\mu)$  mode, and  $\hat{I}$  and  $\hat{C}_{-m}$  are the  $3 \times 3$  unit matrix and a matrix whose elements

are Clebsch–Gordan coefficients, respectively. The normal modes and frequencies of  $C_{60}$  are used for  $C_{60}^-$ , so the higher vibronic terms which mix the normal modes of fullerene are neglected. As a  $T_{1u}$  electronic basis set  $\{|m_{el}\rangle; m_{el} = -1, 0, 1\}$  and normal coordinates of the  $h_g$  modes  $\{Q_{h_g(\mu)m}; m = -2, -1, 0, 1, 2\}$ , we use complex basis which transform as spherical harmonics  $\{Y_{1m_{el}}; m_{el} = -1, 0, 1\}$  and  $\{Y_{2m}; m = -2, -1, 0, 1, 2\}$ , respectively, under the rotations.<sup>16,17</sup> Then  $\hat{I}$  and  $\hat{C}_{-m}$  are written as<sup>18</sup>

$$\begin{aligned} \hat{I} &= \begin{pmatrix} 1 & 0 & 0 \\ 0 & 1 & 0 \\ 0 & 0 & 1 \end{pmatrix}, & \hat{C}_{-2} &= \begin{pmatrix} 0 & 0 & \sqrt{\frac{3}{5}} \\ 0 & 0 & 0 \\ 0 & 0 & 0 \end{pmatrix}, \\ \hat{C}_{-1} &= \begin{pmatrix} 0 & -\sqrt{\frac{3}{10}} & 0 \\ 0 & 0 & \sqrt{\frac{3}{10}} \\ 0 & 0 & 0 \end{pmatrix}, & \hat{C}_0 &= \begin{pmatrix} \frac{1}{\sqrt{10}} & 0 & 0 \\ 0 & \frac{-2}{\sqrt{10}} & 0 \\ 0 & 0 & \frac{1}{\sqrt{10}} \end{pmatrix}, \\ \hat{C}_1 &= \begin{pmatrix} 0 & 0 & 0 \\ \sqrt{\frac{3}{10}} & 0 & 0 \\ 0 & -\sqrt{\frac{3}{10}} & 0 \end{pmatrix}, & \hat{C}_2 &= \begin{pmatrix} 0 & 0 & 0 \\ 0 & 0 & 0 \\ \sqrt{\frac{3}{5}} & 0 & 0 \end{pmatrix}. \end{aligned} \quad (3)$$

This type of the Jahn–Teller problem was investigated by O’Brien<sup>19</sup> and the vibronic coupling constants defined by her are often used. Thus we introduce the coefficient  $\sqrt{5}/2$  in front of the vibronic term to make  $V_{h_g}$  the same as O’Brien’s coupling constants.

Since the linear  $T_{1u} \otimes (2a_g \oplus 8h_g)$  Jahn–Teller Hamiltonian (2) commutes with squared vibronic angular momentum  $\mathbf{J}$  and the  $z$  component of  $\mathbf{J}$ ,<sup>20</sup> the eigenstate of the Hamiltonian (2) is the simultaneous eigenstate of the vibronic angular momentum  $J$ , the  $z$  component of the vibronic angular momentum  $M$ . Here, the vibronic angular momentum  $\mathbf{J}$  is the sum of the vibrational angular momentum  $\mathbf{L}$  and the “energy spin”  $\mathbf{S}$  describing the threefold orbital degeneracy ( $S = 1$ ).<sup>20</sup> In the case of linear vibronic coupling, the eigenstate of  $H$  is the product of the  $T_{1u} \otimes (8h_g)$  Jahn–Teller part and the  $a_g$  vibrational part. As a vibronic basis a set of the products of electronic states and vibrational states of the  $a_g$  and  $h_g$  modes is used:

$$\{|m_{el}\rangle | \cdots \mathbf{n}_\mu \cdots \rangle |v_1 v_2\rangle_{a_g}\}. \quad (4)$$

Here,  $\mathbf{n}_\mu$  means a set of vibrational quantum numbers of the  $h_g(\mu)$  mode,  $\mathbf{n}_\mu = \{n_{\mu m}\}$ ,  $v_1, v_2$  are vibrational quantum numbers of the  $a_g(1)$  mode and the  $a_g(2)$  mode respectively. Then the eigenstate  $|\Psi_{v_1 v_2 k J M}\rangle$  of the Hamiltonian (2) which belongs to the eigenvalue  $\sum_{i=1}^2 [\hbar\omega_{a_g(i)} v_i - V_{a_g(i)}^2 / (2\omega_{a_g(i)}^2)] + E_{kJ}$  is represented as a linear combination of the vibronic basis with con-

stants  $C_{m_{el}, \mathbf{n}_1 \cdots \mathbf{n}_8; k J M}^{\text{JT}}$ .

$$\begin{aligned} |\Psi_{v_1 v_2 k J M}\rangle &= \sum_{m_{el}=-1}^1 \sum_{\mathbf{n}_1} \cdots \sum_{\mathbf{n}_8} |m_{el}\rangle | \mathbf{n}_1 \cdots \mathbf{n}_8 \rangle \\ &\times C_{m_{el}, \mathbf{n}_1 \cdots \mathbf{n}_8; k J M}^{\text{JT}} \\ &\times \sum_{v'_1=0}^{\infty} \sum_{v'_2=0}^{\infty} |v'_1 v'_2\rangle_{a_g} S_{v'_1 v_1}(g_{a_g(1)}) S_{v'_2 v_2}(g_{a_g(2)}), \end{aligned} \quad (5)$$

where  $E_{kJ}$  is an eigenvalue of the  $T_{1u} \otimes (8h_g)$  Jahn–Teller Hamiltonian,  $k$  distinguishes energy levels with the same  $J$  and  $M$ , the dimensionless VCC of the  $\Gamma(\mu)$  mode  $g_{\Gamma(\mu)}$  ( $\Gamma = a_g, h_g$ ) is defined as

$$g_{\Gamma(\mu)} = \frac{V_{\Gamma(\mu)}}{\sqrt{\hbar\omega_{\Gamma(\mu)}^3}}, \quad (6)$$

the Franck–Condon factor of the  $a_g$  mode  $S_{v'v}(g)$  is written as

$$S_{v'v}(g) = \sqrt{\frac{v!v!}{2^{v'-v}}} e^{-\frac{1}{2}g^2} \sum_{l=l_{\min}}^v \left(-\frac{1}{2}\right)^l \frac{g^{2l+v'-v}}{l!(v-l)!(v'-v+l)!}, \quad (7)$$

$l_{\min} = 0$  for  $v \leq v'$ , and  $l_{\min} = v - v'$  for  $v > v'$ . The origin of the energy is the lowest energy of  $C_{60}^-$  without vibronic couplings.

To obtain the vibronic states, we diagonalize the linear  $T_{1u} \otimes 8h_g$  Jahn–Teller Hamiltonian numerically using Lanczos method. We use a truncated vibronic basis set,

$$\left\{ |m_{el}\rangle | \cdots \mathbf{n}_\mu \cdots \rangle; \sum_{\mu=1}^8 \sum_{m=-2}^2 n_{\mu m} \leq N \right\}. \quad (8)$$

Here,  $N$  is the maximum number of the vibrational excitations in the vibronic basis set (8). We treat the vibronic states which  $J$ s are from 0 to 7. Frequencies  $\omega_{a_g(i)}, \omega_{h_g(\mu)}$  are taken from the experimental frequencies of Raman scattering in solid state  $C_{60}$ .<sup>21</sup>

Lastly, we introduce stabilization energies which we use to show our results. The stabilization energy of each mode is defined as

$$E_{s,i} = \frac{V_{a_g(i)}^2}{2\omega_{a_g(i)}^2}, \quad (9)$$

$$E_{\text{JT},\mu} = \frac{V_{h_g(\mu)}^2}{2\omega_{h_g(\mu)}^2}, \quad (10)$$

and the total stabilization energies of the  $a_g$  modes and  $h_g$  modes are

$$E_s = \sum_{i=1}^2 E_{s,i}, \quad (11)$$

$$E_{\text{JT}} = \sum_{\mu=1}^8 E_{\text{JT},\mu}. \quad (12)$$

They represent the depth of the potential energy surface from the energy of undistorted fullerene monoanion.

### III. SIMULATION OF THE PHOTOELECTRON SPECTRUM

The photoelectron spectrum is simulated within the sudden approximation.<sup>22</sup> We assume that each  $C_{60}^-$  is

$$I(\Omega) \propto \sum_{k,J} \sum_{v'_1, v'_2} p_{v'_1} p_{v'_2} p_{k,J} \sum_{m_{el}=-1}^1 |C_{m_{el}, \mathbf{n}_1 \dots \mathbf{n}_8; k, J, 0}^{JT} S_{v'_1 v_1}(g_{a_g(1)}) S_{v'_2 v_2}(g_{a_g(2)})|^2 \times \delta \left[ \frac{E_0 + E_s - E_{k,J}}{\hbar} + \sum_{\mu=1}^8 \sum_{m=-2}^2 \omega_{h_g(\mu)} n_{\mu m} + \sum_{i=1}^2 \omega_{a_g(i)} (v_i - v'_i) - \Omega \right], \quad (13)$$

where,  $p_{v_i}$  and  $p_{k,J}$  are the statistical weights of the  $a_g(i)$  mode and the Jahn–Teller part, respectively,

$$p_{v_i} = \frac{1}{Z_{a_g}} \exp(-\hbar \omega_{a_g(i)} v_i \beta), \quad (14)$$

$$p_{k,J} = \frac{2J+1}{Z_{JT}} \exp(-E_{k,J} \beta), \quad (15)$$

$Z_{a_g}$  and  $Z_{JT}$  are corresponding statistical sums, and  $E_0$  is the gap between the ground electronic energies of  $C_{60}$  and  $C_{60}^-$ . The envelope function is represented by using the Gaussian function with the standard deviation  $\sigma$ :

$$F(\Omega) = \int_{-\infty}^{\infty} I(\Omega') \exp\left[-\frac{(\Omega - \Omega')^2}{2\sigma^2}\right] d\Omega'. \quad (16)$$

For a decent simulation of experimental PES one should include in Eq. (16), in principle, also the contributions from the rotational spectrum of  $C_{60}^-$ . However, due to a large momentum of inertia of fullerene and restrictive selection rules for the transitions between different rotational levels<sup>23</sup> our estimations gave an expected enlargement of the transition band of only several wave numbers. This is negligible compared the full width at half maximum (FWHM) given by the envelope function (16).

To evaluate the agreement between the simulated spectrum and the experimental spectrum, we calculate the residual of theoretical spectrum  $F_{\text{calc}}(\Omega)$  and the experimental spectrum  $F_{\text{exp}}(\Omega)$ . The residual  $R$  is defined by the equation:

$$R = \min_{f, \Omega_{\text{shift}}} \left\{ \frac{\sum_{i=0}^M [F_{\text{calc}}(\Omega_i) - f F_{\text{exp}}(\Omega_i - \Omega_{\text{shift}})]^2}{\sum_{j=0}^M F_{\text{calc}}^2(\Omega_j)} \right\}. \quad (17)$$

Here,  $f$  is the parameter to vary the height,  $\Omega_{\text{shift}}$  is the parameter to shift the experimental spectrum,  $\Omega_i$  is a sampling point. The minimum and maximum of  $\Omega_i$  is  $\Omega_{\text{min}}$  and  $\Omega_{\text{max}}$ , and the gap between adjacent sampling points  $\Delta\Omega$  is constant. Then  $M$  is represented as  $M = (\Omega_{\text{max}} - \Omega_{\text{min}})/\Delta\Omega$  and  $\Omega_i = \Omega_{\text{min}} + i\Delta\Omega$ . In the calculation of the residual  $R$ ,  $\Omega_{\text{min}}$ ,  $\Omega_{\text{max}}$ , and  $\Delta\Omega$  are  $-200 \text{ cm}^{-1}$ ,  $1600 \text{ cm}^{-1}$ , and  $0.5 \text{ cm}^{-1}$  respectively. We

in a thermal equilibrium state, hence we use a Boltzmann's distribution to calculate the statistical weight. With these assumptions, the intensity of the transition which appears at the binding energy  $\hbar\Omega$  is written as follows:

avoid the truncation of the zero phonon line of Gunnarsson *et al.*<sup>3</sup> VCCs are varied in order to make  $R$  as small as possible within the accuracy of the experiment. The accuracy is determined from the range of the vibrational temperature of  $C_{60}^-$  in the experiment of Wang *et al.*<sup>15</sup> In their experiment, the vibrational temperature is between 70 K and 90 K. Although the shapes of the simulated spectra at 70 K and 90 K are different from each other, we cannot distinguish them from the experiment of Wang *et al.* In terms of the residual  $R$ , the difference between  $R$  at 70 K and  $R$  at 90 K is practically indistinguishable.

### IV. DFT CALCULATION OF VIBRONIC COUPLING CONSTANTS

The linear vibronic coupling constant of the  $a_g(i)$  mode is a diagonal matrix element of the first derivative of the electronic Hamiltonian with respect to the normal coordinate at the reference geometry.<sup>20</sup>

$$V_{a_g(i)} = \langle \psi | \left( \frac{\partial H_{\text{el}}(\mathbf{R})}{\partial Q_{a_g(i)}} \right)_{\mathbf{R}_0} | \psi \rangle, \quad (18)$$

where  $\psi$  is the ground electronic state. By applying the Hellmann–Feynman theorem<sup>24</sup> to Eq. (18) and then transforming it into the formula with the vibrational vector, we obtain

$$V_{a_g(i)} = \left( \frac{\partial E(\mathbf{R})}{\partial Q_{a_g(i)}} \right)_{\mathbf{R}_0} \quad (19)$$

$$= \sum_{A=1}^{60} \left( \frac{\partial E(\mathbf{R})}{\partial \mathbf{R}_A} \right)_{\mathbf{R}_0} \cdot \frac{\mathbf{u}_A^{a_g(i)}}{\sqrt{M}}. \quad (20)$$

Here,  $A$  indicates a carbon atom in  $C_{60}$ ,  $\mathbf{R}_A$  is the Cartesian coordinate of  $A$ ,  $\mathbf{R}$  is the set of all  $\mathbf{R}_A$ ,  $H_{\text{el}}(\mathbf{R})$  is the electronic Hamiltonian at the structure  $\mathbf{R}$ ,  $\mathbf{R}_0$  is the reference nuclear configuration,  $E(\mathbf{R})$  is the ground electronic energy  $\langle \psi | H_{\text{el}}(\mathbf{R}) | \psi \rangle$ ,  $M$  is the mass of carbon atom,  $\mathbf{u}_A^{a_g(i)}$  is the vibrational vector of the  $a_g(i)$  mode. Similarly, absolute value of the coupling constant of the

$h_g(\mu)$  mode is written as

$$V_{h_g(\mu)} = \sqrt{\sum_{m=-2}^2 \left( \frac{\partial E(\mathbf{R})}{\partial Q_{h_g(\mu)m}} \right)_{\mathbf{R}_0}^2} \quad (21)$$

$$= \sqrt{\sum_{m=-2}^2 \left[ \sum_{A=1}^{60} \left( \frac{\partial E(\mathbf{R})}{\partial \mathbf{R}_A} \right)_{\mathbf{R}_0} \cdot \frac{\mathbf{u}_A^{h_g(\mu)m}}{\sqrt{M}} \right]^2} \quad (22)$$

The equilibrium geometry  $\mathbf{R}_0$ , the vibrational vectors  $\mathbf{u}_{a_g(i)}$ ,  $\mathbf{u}_{h_g(\mu)m}$ , and the gradient of the electronic energy  $(\partial E(\mathbf{R})/\partial \mathbf{R}_A)_{\mathbf{R}_0}$ , entering the Eqs. (20) and (22), are obtained from *ab initio* calculations. Note that the vibronic coupling constants (19), (21) are not equal to the gradients of the frontier levels (see Appendix).

We compute the VCCs of  $C_{60}^-$  using the DFT method. As exchange-correlation functional, the hybrid functional of Becke<sup>25</sup> (B3LYP) is used. To find VCCs which are close to the experimental results the fraction of the Hartree-Fock exchange energy are varied from the original fraction 20% to 30% by 5%. We use the triple zeta basis sets, 6-311G(d), 6-311+G(d), and cc-pVTZ.

The structure optimization and the calculation of the vibrational modes are performed for the neutral fullerene. The electronic wavefunction of  $C_{60}^-$  are obtained from the variational calculation of an unrestricted Slater determinant. As far as the method based on the single determinant is used, the spatial symmetry of the wavefunction is broken and the degeneracy of the singly occupied degenerate level is lifted.<sup>26,27</sup> However, in the case of the cyclopentadienyl radical, it was demonstrated that the splitting of the total electronic energies estimated by the unrestricted B3LYP method is only 0.4 meV.<sup>26,27</sup> It is expected that the splitting of the  $T_{1u}$  ground electronic energies of  $C_{60}^-$  is tiny and the symmetry of the electronic state may not be broken significantly. Thus we treat the wavefunction as a  $T_{1u}$  wavefunction. We calculate the energy gradient  $\partial E(\mathbf{R})/\partial \mathbf{R}_A|_{\mathbf{R} \rightarrow \mathbf{R}_0}$  with the coupled perturbed Kohn-Sham method. In the calculation of the dimensionless VCCs (6) and the stabilization energies (10), we use the experimental frequencies.<sup>21</sup> To compute electronic structures we use the Gaussian 03 program.<sup>28</sup>

## V. DERIVATION OF THE VIBRONIC COUPLING CONSTANTS OF $a_g$ MODES FROM THE STRUCTURES OF $C_{60}$ AND $C_{60}^-$

We also derive the stabilization energies of the  $a_g$  modes from the experimental bond lengths of  $C_{60}$  and  $C_{60}^-$ . The structures of  $C_{60}$  and  $C_{60}^-$  with  $I_h$  symmetry are determined by the C-C bond lengths of the edges between two hexagons (6:6) and a hexagon and pentagon (6:5). We use average 6:6 and 6:5 C-C bond lengths of TDAE- $C_{60}$  for  $C_{60}^-$  and fullerite for  $C_{60}$ . The data of TDAE- $C_{60}$  are obtained from the results of X-ray diffraction at 7K by Narymbetov *et al.*<sup>29</sup> and at 25K and 90K

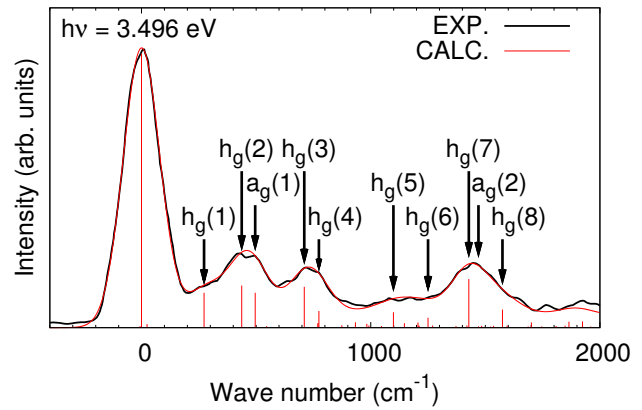


FIG. 1. The photoelectron spectrum measured by Wang *et al.* (black line) and the simulated spectrum (red line). The simulation is performed at 70 K with  $\sigma = 80 \text{ cm}^{-1}$ .

by Fujiwara *et al.*<sup>30</sup>. The average bond lengths of fullerite are taken from the results of neutron diffraction at 5K by David *et al.*<sup>31</sup> and X-ray diffraction at 110K by Bürgi *et al.*<sup>32</sup> To remove the thermal expansion of the C-C bond lengths, we use sets of bond lengths of  $C_{60}$  and  $C_{60}^-$  which are measured at close temperature. That is, the bond lengths of  $C_{60}$  measured at 5K is used with the bond lengths of  $C_{60}^-$  measured at 7K and 25K, and the bond lengths of  $C_{60}$  at 110K is used with the bond lengths of  $C_{60}^-$  at 90K. The vibronic coupling constants of the  $a_g$  modes  $V_{a_g(i)}$  ( $i = 1, 2$ ) are obtained from the equation

$$V_{a_g(i)} = - \sum_{A=1}^{60} (\mathbf{R}_A - \mathbf{R}_{0,A}) \cdot \frac{\mathbf{u}_A^{a_g(i)}}{\sqrt{M}}. \quad (23)$$

To perform the calculation, we use the vibrational vector defined in the calculations with the B3LYP method and the cc-pVTZ basis.

## VI. RESULTS AND DISCUSSIONS

### A. Simulation of the PES of Wang *et al.*

We simulate the photoelectron spectrum measured by Wang *et al.*<sup>15</sup> at 70 K. The basis set in Eq. (5) includes up to 6 vibrational excitations ( $N = 6$ ). The experimental and simulated spectra are shown in Fig. 1. The transition between the ground states of  $C_{60}^-$  and  $C_{60}$  (the 0-0 line)<sup>33</sup> is chosen as the origin of these spectra. From the spectrum of Wang *et al.*, we obtain several sets of VCCs listed as (1), (2), and (3) in Tables I and II. We extracted  $\sigma = 80 \text{ cm}^{-1}$  by fitting the FWHM of the 0-0 line ( $188 \text{ cm}^{-1}$ ). The increase or decrease of the  $\sigma$  makes the agreement between the simulated and experimental spectra worse.

TABLE I. Absolute values of dimensionless vibronic coupling constants obtained in the present work.

	Frequency ( $\text{cm}^{-1}$ )	PES					B3LYP <sup>c</sup>						
		Wang <sup>a</sup>		Gunnarsson <sup>b</sup>			6-311G(d)			6-311+G(d)		cc-pVTZ	
		(1)	(2)	(3)	(4)	(5)	20 %	25 %	30 %	20 %	20 %	25 %	
$a_g(1)$	496	0.505	0.505	0.500	0.141	0.505	0.287	0.272	0.269	0.346	0.289	0.286	
$a_g(2)$	1470	0.100	0.200	0.300	0.424	0.200	0.415	0.445	0.460	0.455	0.430	0.450	
$h_g(1)$	273	0.500	0.500	0.490	0.740	0.820	0.436	0.437	0.444	0.426	0.442	0.452	
$h_g(2)$	437	0.525	0.520	0.515	0.860	0.690	0.498	0.504	0.508	0.479	0.498	0.494	
$h_g(3)$	710	0.465	0.460	0.455	0.390	0.350	0.418	0.464	0.476	0.412	0.403	0.414	
$h_g(4)$	774	0.310	0.310	0.300	0.490	0.490	0.259	0.241	0.243	0.252	0.273	0.283	
$h_g(5)$	1099	0.285	0.280	0.280	0.320	0.300	0.211	0.233	0.241	0.211	0.212	0.217	
$h_g(6)$	1250	0.220	0.230	0.235	0.190	0.160	0.126	0.169	0.178	0.126	0.125	0.124	
$h_g(7)$	1428	0.490	0.470	0.435	0.320	0.430	0.398	0.414	0.433	0.392	0.398	0.415	
$h_g(8)$	1575	0.295	0.285	0.260	0.350	0.410	0.338	0.335	0.345	0.330	0.333	0.343	

<sup>a</sup> (1),(2),and (3) are derived from the PES of Wang *et al.* (Ref. 15)

<sup>b</sup> (4),(5) are derived from the PES of Gunnarsson *et al.* (Ref. 3)

<sup>c</sup> The percentage 20 %, 25 %, and 30 % indicate fractions of the Hartree–Fock exact exchange taken in the exchange–correlation functional.

TABLE II. Stabilization energies (meV) obtained in the present work.

	Frequency ( $\text{cm}^{-1}$ )	PES					B3LYP <sup>c</sup>						
		Wang <sup>a</sup>		Gunnarsson <sup>b</sup>			6-311G(d)			6-311+G(d)		cc-pVTZ	
		(1)	(2)	(3)	(4)	(5)	20 %	25 %	30 %	20 %	20 %	25 %	
$a_g(1)$	496	7.8	7.8	7.7	0.6	7.8	2.5	2.3	2.2	3.7	2.6	2.5	
$a_g(2)$	1470	0.9	3.6	8.2	16.4	3.6	15.7	18.0	19.3	18.9	16.9	18.5	
$h_g(1)$	273	4.2	4.2	4.1	9.3	11.4	3.2	3.2	3.3	3.1	3.3	3.5	
$h_g(2)$	437	7.5	7.3	7.2	20.0	12.9	6.7	6.9	7.0	6.2	6.7	6.6	
$h_g(3)$	710	9.5	9.3	9.1	6.7	5.4	7.7	9.5	10.0	7.5	7.2	7.6	
$h_g(4)$	774	4.6	4.6	4.3	11.5	11.5	3.2	2.8	2.8	3.1	3.6	3.8	
$h_g(5)$	1099	5.5	5.3	5.3	7.0	6.1	3.0	3.7	4.0	3.0	3.0	3.2	
$h_g(6)$	1250	3.9	4.1	4.3	2.8	2.0	1.2	2.2	2.5	1.2	1.2	1.2	
$h_g(7)$	1428	21.3	19.6	16.8	9.1	16.4	14.0	15.2	16.6	13.6	14.0	15.2	
$h_g(8)$	1575	8.5	7.9	6.6	12.0	16.4	11.2	11.0	11.6	10.7	10.9	11.5	
$E_s$		8.7	11.4	15.9	17.0	11.4	18.2	20.3	21.5	22.6	19.5	21.0	
$E_{\text{JT}}$		65.0	62.3	57.7	78.4	82.1	50.2	54.4	57.8	48.4	49.9	52.6	
$E_s + E_{\text{JT}}$		73.7	73.7	73.6	95.4	93.5	68.4	74.7	79.3	71.0	69.4	73.6	

<sup>a</sup> (1),(2),and (3) are derived from the PES of Wang *et al.* (Ref. 15)

<sup>b</sup> (4),(5) are derived from the PES of Gunnarsson *et al.* (Ref. 3)

<sup>c</sup> The percentage 20 %, 25 %, and 30 % indicate fractions of the Hartree–Fock exact exchange taken in the exchange–correlation functional.

To assess the thermal population of the excited vibronic states, we calculate statistical weights of the excited Jahn–Teller levels  $p_{kJ}$  at 70 K and 90 K. The vibronic levels are obtained using the set of VCCs (1). In the calculation of the distribution function  $Z_{\text{JT}}$ , we include all excited vibronic levels whose weights are larger than  $10^{-7}$ . The computed weights are shown in Table III. Although these statistical weights are computed us-

ing the set (1), rest of the sets of VCCs (2), (3) give similar results. The statistical weights of the ground vibronic level at 70 K and 90 K are more than 90 %. This indicates that the transition from the ground vibronic level is dominant in the PES of Wang *et al.* We focus, therefore, on the ground vibronic level to discuss the effect of the size of the basis (8) on the calculated vibronic states. The ground vibronic level is  $-962.65 \text{ cm}^{-1}$  when

TABLE III. The lowest vibronic levels ( $\text{cm}^{-1}$ ) and the statistical weights  $p_{k,J}$  (%) at 70 K and 90 K.  $J$  is the magnitude of the vibronic angular momentum. To calculate the vibronic levels, the set of VCCs (1) in Table I is used.

Level	$J$	Energy	Weight	
			70 K	90 K
1	1	-962.85	97.75	92.48
2	3	-713.97	1.37	4.04
3	2	-683.40	0.52	1.77
4	1	-672.75	0.25	0.90
Sum			99.89	99.19

TABLE IV. Residuals of the experimental and simulated spectra. The calculation of the residual is performed for all sets of VCCs in Table I at 70 K and 90 K.

	Set (1)		Set (2)		Set (3)	
	70 K	90 K	70 K	90 K	70 K	90 K
$R \times 10^{-4}$	8.35	8.07	8.41	8.16	8.76	8.41

we use the basis set with  $N = 5$ . Compared with the gap between the ground and first excited vibronic levels with  $J = 1$ , the change of the ground vibronic level due to the increase of the size of the vibronic basis set is only about 0.07 %. Therefore, we regard our basis set as large enough to simulate the spectrum of Wang *et al.*

The differences between several sets of VCCs are in the constants of  $a_g(2)$ ,  $h_g(7)$ , and  $h_g(8)$  modes. If we increase the dimensionless VCC (the stabilization energy) of the  $a_g(2)$  mode from 0.1 to 0.3 (0.9 to 8.2 meV) and at the same time decrease the dimensionless VCCs of  $h_g(7)$ ,  $h_g(8)$  modes, the shape of the PES does not vary significantly (see Fig. 2). This is due to a poor resolution of the peaks of  $a_g(2)$ ,  $h_g(7)$ , and  $h_g(8)$  modes and essentially the same problem arose in the analysis of Gunnarsson *et al.*<sup>3</sup> In the latter case, the stabilization energy of  $a_g(2)$  is varied from 0 to 45 meV, i.e., in a range larger than ours. Owing to the narrow peaks of the spectrum of Wang *et al.*, we can derive the VCCs with less ambiguity.

We compute the residuals (17) of the experimental and the simulated spectra for all sets of VCCs at 70 K and 90 K. The values are shown in Table IV. The differences of the residuals of the different sets of VCCs are almost within the ambiguity of the vibrational temperature. Therefore, we conclude that these sets of VCCs cannot be distinguished from the experiment of Wang *et al.*

Although we obtain several sets of VCCs, the stabilization energies  $E_s + E_{JT}$  are similar to each other (see (1), (2), and (3) in Table II). On the other hand, present stabilization energies are smaller than the stabilization energy of Gunnarsson *et al.*<sup>3</sup> by 30 % (see Table V), i.e., the Jahn–Teller coupling is weaker than previously expected.

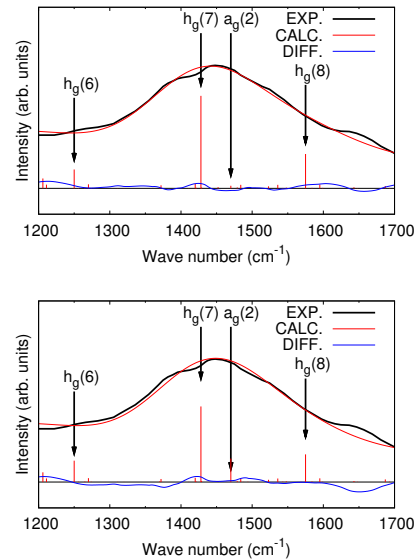


FIG. 2. The peak of the photoelectron spectra due to  $a_g(2)$ ,  $h_g(7)$ , and  $h_g(8)$  modes. The black line indicates the experimental spectrum of Wang *et al.*,<sup>15</sup> the red line indicates the simulated spectrum, and the blue line indicates the difference between the experimental and simulated spectra. The top of the two spectra is simulated using the VCCs (1) and the bottom one is simulated using the VCCs (3) from Table I. The simulation is performed at 70 K with  $N = 6$  and  $\sigma = 80 \text{ cm}^{-1}$ .

We find that the distributions of  $E_{s,i}$  and  $E_{JT,\mu}$  also differ from each other (Tables II, V). In Ref. 3, the stabilization energy of  $h_g(2)$  was found the strongest, while our results show that the strongest is the stabilization energy of  $h_g(7)$ .

Hands *et al.* estimated the Jahn–Teller stabilization energy  $E_{JT}$  of 57.94 meV within the single-mode  $T_{1u} \otimes h_g$  Jahn–Teller model from the visible and near-infrared spectrum.<sup>5</sup> The present Jahn–Teller stabilization energy agrees well with their value.

## B. Simulation of the PES of Gunnarsson *et al.*

As a preliminary calculation, we compute the vibronic levels using the data from Ref. 3, that is, the same VCCs and the same size of the vibronic basis ( $N = 5$ ). The statistical weight of the ground state at 200 K is obtained ca. 39 %. This result indicates that not only the ground level but also excited levels must be considered in order to simulate the spectrum of Gunnarsson *et al.*<sup>3</sup>

We simulate this spectrum at 200 K with the FWHM of  $283 \text{ cm}^{-1}$  ( $\sigma = 120 \text{ cm}^{-1}$ ). The size of the vibronic basis set is  $N = 7$ . The experimental and the simulated spectra are shown in Fig. 3. As was mentioned also by Gunnarsson *et al.*,<sup>3</sup> we obtain several sets of VCCs that give close stabilization energies. These sets of dimensionless VCCs and stabilization energies are (4), (5) in Table

TABLE V. Comparison between the obtained stabilization energies of  $C_{60}^-$  with previous results (meV).

	Freq. ( $\text{cm}^{-1}$ )	PES		LDA		GGA	MNDO	B3LYP		(10) <sup>a</sup>
		(3) <sup>a</sup>	Gun <sup>3</sup>	Man <sup>11</sup>	Bre <sup>10</sup>	Fre <sup>13</sup>	Var <sup>6 b</sup>	Sai <sup>12 b</sup>	Laf <sup>14</sup>	
$a_g(1)$	496	7.7	0.6	0.2	1.5	1.5	-	-	1.8	2.6
$a_g(2)$	1470	8.2	16.4	2.7	9.0	11.0	-	-	16.4	16.9
$h_g(1)$	273	4.1	11.4	2.7	6.0	2.8	1.8	3.6	3.5	3.3
$h_g(2)$	437	7.2	24.0	6.3	15.6	7.0	0.6	6.6	6.5	6.7
$h_g(3)$	710	9.1	7.8	5.5	6.6	6.1	0.6	6.6	7.1	7.2
$h_g(4)$	774	4.3	10.8	2.4	3.0	2.4	0.0	3.0	3.1	3.6
$h_g(5)$	1099	5.3	7.2	2.6	3.6	2.6	3.6	3.0	3.0	3.0
$h_g(6)$	1250	4.3	3.0	1.5	1.8	1.9	0.0	1.8	1.3	1.2
$h_g(7)$	1428	16.8	10.2	9.0	9.6	9.0	20.4	13.2	13.8	14.0
$h_g(8)$	1575	6.6	13.8	8.2	4.8	8.8	6.6	10.2	10.6	10.9
$E_s$		15.9	17.0	2.9	10.5	12.5	-	-	18.2	19.5
$E_{JT}$		57.7	88.2	38.2	51.0	40.6	33.6	48.0	48.9	49.9
$E_s + E_{JT}$		73.6	105.2	41.1	61.5	53.1	-	-	67.1	69.4

<sup>a</sup> Results given in Tables II.

<sup>b</sup> The stabilization energies of the  $a_g$  modes are not reported.

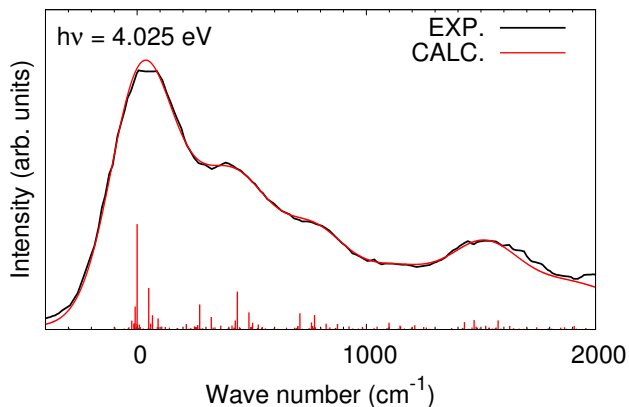


FIG. 3. The experimental photoelectron spectrum measured by Gunnarsson *et al.*<sup>3</sup> (black line) and the simulated spectrum (red line). The simulation is performed at 200 K with  $\sigma = 120 \text{ cm}^{-1}$ .

I and II respectively. In comparison with the original stabilization energy of Gunnarsson *et al.*, present stabilization energies are smaller by 10 meV. However, stabilization energies are still larger than those obtained from the spectrum of Wang *et al.* by 20 meV. The inconsistencies of these VCCs come from the difference between the shapes of the spectra of Wang *et al.* and Gunnarsson *et al.*, due to different vibrational temperature and resolution.

Simulating the spectrum of Gunnarsson *et al.*, we encounter two problems. First, the spectrum is too broad and, second, the vibrational temperature is too high. In fact, the statistical weights of the ground vibronic level at 200 K are about 37 % in both cases (see Table VI),

hence, we must consider many excited vibronic states. To represent the excited vibronic states with enough accuracy, we expect that the vibronic basis must be larger than the present one. Furthermore, as the vibrational temperature is further increased, the weight of each vibronic level and the shape of the spectrum varies easily. Although the range of the vibrational temperature is not reported, we increased the temperature by 20 K which is the uncertainty range of vibrational temperature in the case of Wang *et al.*<sup>15</sup> The statistical weights of the ground vibronic level decreased from ca. 37 % to ca. 31 % with this increase of the temperature. This change of the weight affects the shape of the spectrum. Therefore it is difficult to perform an accurate simulation and to estimate VCCs from the spectrum of Gunnarsson *et al.*

Given better the experimental conditions of Wang *et al.*<sup>15</sup> allowing for more accurate simulations, we may conclude that the VCCs extracted from these experiments should be considered more reliable than those obtained by Gunnarsson *et al.*<sup>3</sup>

### C. DFT calculations of the vibronic coupling constants

We compute the vibronic coupling constants of  $C_{60}^-$  using the DFT method described in Sec. IV. For DFT calculations with pure functionals, it is well known that in the high-symmetry geometry the occupied level belonging to one degenerate representation moves upwards in energy relative to the empty levels belonging to the same degenerate manifold.<sup>34</sup> However in our case the situation is opposite (the occupied level is the lowest one) because of the Hartree-Fock exchange contribution contained in the B3LYP functional. The splitting between

TABLE VI. The computed vibronic levels ( $\text{cm}^{-1}$ ) and statistical weights  $p_{k,J}$  (%) using the sets of VCCs (4), (5) which are derived from the experimental spectrum of Gunnarsson *et al.*<sup>3</sup> The statistical weights are calculated at 200K.

Level	Set (4)			Set (5)		
	$J$	Energy	Weight 200 K	$J$	Energy	Weight 200 K
1	1	-1067.6	36.56	1	-1134.4	37.00
2	3	-845.2	17.22	3	-914.7	17.77
3	2	-785.9	8.03	2	-850.2	7.98
4	1	-771.3	4.34	1	-829.9	4.14
5	3	-697.5	5.95	3	-742.5	5.15
6	2	-616.0	2.37	2	-687.8	2.48
7	5	-613.1	5.10	5	-685.5	5.37
8	1	-590.0	1.18	1	-667.0	1.28
9	3	-580.3	2.56	3	-650.1	2.65
10	2	-535.1	1.32	2	-595.0	1.27
11	4	-531.4	2.06	4	-594.0	2.02
12	1	-525.4	0.74	1	-590.6	0.74
13	3	-485.2	1.29	3	-543.5	1.23
14	5	-464.8	1.75	5	-515.2	1.58
15	4	-445.7	1.11	4	-495.6	1.00
16	2	-404.6	0.52	2	-456.7	0.47
17	7	-371.4	1.22	7	-446.6	1.31
18	4	-362.7	0.61	3	-436.7	0.57
19	3	-362.1	0.53	4	-432.7	0.63
20	5	-339.6	0.71	5	-414.8	0.77
21	0	-330.5	0.06	0	-400.2	0.06
22	2	-317.4	0.28	4	-388.3	0.46
23	4	-316.8	0.44	2	-387.9	0.29
24	1	-291.3	0.14	1	-357.6	0.14
25	6	-275.4	0.53	6	-336.5	0.52
Sum			96.62			96.88

TABLE VII. The splitting between the lifted one-electron  $t_{1u}$  levels  $\Delta\epsilon$  (meV).

$\Delta\epsilon$	6-311G(d)			6-311+G(d)	cc-pVTZ	
	20 %	25 %	30 %	20 %	20 %	25 %
	691	874	1059	686	693	876

the  $t_{1u}$  Kohn–Sham levels are about 1 eV (see Table VII) and the variations of the total electronic energies for different occupation schemes of  $t_{1u}$  orbitals are less than 0.2 meV. Moreover, the vibronic coupling constants do not depend on the choice of the electronic states significantly. The variation of the total stabilization energy is ca. 1 meV. The dimensionless VCCs and the stabilization energies are shown in Table I and II. Although we use several basis sets, the VCCs do not depend on the basis set significantly. On the other hand, the VCCs

vary with the increase of the fraction of the Hartree–Fock exchange energy in the exchange–correlation functional. Increasing this fraction leads to larger VCCs and stabilization energies. We find that the stabilization energies of high frequency modes,  $a_g(2)$ ,  $h_g(7)$ , and  $h_g(8)$  are the strongest. Compared with other DFT calculations, we may conclude that the stabilization energies of  $a_g$  modes agree well with the previous calculations, while the present stabilization energy  $E_s + E_{JT}$  is larger than the previous results.

In comparison with present simulation of the experimental PES, the DFT calculations with the energy functionals including fractions of 20 % and 25 % of the Hartree–Fock exchange energy give close values. Although the stabilization energy  $E_s + E_{JT}$  obtained using the original B3LYP functional is slightly smaller than the experimental value, the result obtained with it is also close to the experimental one. The distribution of the computed stabilization energy of each  $h_g$  mode  $E_{JT,\mu}$  qualitatively agrees with the experimental results. The stabilization energy of the  $h_g(7)$  mode is obtained smaller and that of the  $h_g(8)$  mode is obtained larger than the experimental values. The slight difference between theoretical and experimental results should originate from still inaccurately computed vibrational vectors. Indeed, it was shown that a small mixing of the vibrational vectors in fullerene affects the values of VCCs significantly.<sup>3</sup> Besides the present computational results, the LDA calculation by Manini *et al.*<sup>11</sup> and the GGA calculation by Frederiksen *et al.*<sup>13</sup> give similar relative values for the coupling constants of  $h_g$  modes as the present simulations of PES of Wang *et al.*<sup>15</sup> On the other hand, these calculations give smaller absolute values of the VCCs and of the total stabilization energies than the presently obtained. Contrary to these calculations, the B3LYP calculation by Saito<sup>12</sup> and Laflamme Janssen<sup>14</sup> give close values of VCCs to the present results. However, despite of using the same B3LYP functional, our calculations of VCCs differ from the ones in Refs. 12 and 14 since we used here the derivative of the total energy, which does not coincide with the derivative of the Kohn–Sham orbital energy (see the appendix). The LDA calculation of Breda *et al.*<sup>10</sup> gives the distribution of relative strengths of VCCs which is similar to the results of Gunnarsson *et al.* and do not agree with the values derived here from PES of Wang *et al.* Varma *et al.*<sup>6</sup> computed VCCs using MNDO method, however, the distribution of the stabilization energies is different from the present simulations of experiment and the theoretical values obtained here.

On the contrary, the theoretical stabilization energy of the  $a_g(1)$  mode is too small and that of the  $a_g(2)$  mode is too large compared to  $E_{s,i}$  derived from experiment (Tables I, II). To find the correct order of the corresponding VCCs, we derive the coupling constants of the  $a_g$  modes from the experimental bond lengths as described in Sect. V. The obtained stabilization energies  $E_{s,i}$  are shown in Table VIII. Unfortunately, as we can see,  $E_{s,i}$  depend very strongly on the set of the C–C bond lengths,



TABLE VIII. Stabilization energies (meV) derived from the experimental C-C bond lengths of  $C_{60}$  and  $C_{60}^-$ .

	Frequency ( $\text{cm}^{-1}$ )	Stabilization energies of $a_g$ modes (meV)				
		(3)	(10)	Narymbetov <sup>a</sup>	Fujiwara <sup>a</sup>	Fujiwara <sup>b</sup>
				7K	25K	90K
$a_g(1)$	496	7.7	2.6	8.0	0.1	58.8
$a_g(2)$	1470	8.2	16.9	0.0	7.5	7.0

<sup>a</sup> The structure of  $C_{60}$  is taken from neutron diffraction at 5K (Ref. 31).

<sup>b</sup> The structure of  $C_{60}$  is taken from X-ray diffraction at 110K (Ref. 32).

thus we cannot draw a conclusion about their relative strength. This comes from the fact that we use the structural data measured by different techniques (X-ray and neutron scattering) on different systems (TDAE- $C_{60}$  and fullerite) for  $C_{60}^-$  and  $C_{60}$ , respectively. In both cases, fullerenes should be deformed due to the environment compared with the free  $C_{60}$  molecule. The distortions caused by the crystal fields of  $C_{60}$  in TDAE- $C_{60}$  and fullerite are different from each other. Furthermore, the expected changes in the bond lengths in  $C_{60}$  and  $C_{60}^-$  are within the experimental accuracy of the structural data. Thus, the origin of the discrepancy of the relative strength of VCCs of the  $a_g$  modes between the simulations and DFT calculations remains unclear.

Note that although the values of  $E_{s,i}$  are different from the experimental results, their sum, as well as, the distribution of  $E_{JT,\mu}$  and  $E_s + E_{JT}$  are close to the experimental values. Therefore, we may conclude that the present theoretical method gives improved values of vibronic coupling constants.

## VII. CONCLUSION

In this work, we simulated the PES of Wang *et al.* and derived the vibronic coupling constants of  $C_{60}^-$ . We obtain several sets of VCCs, because the frequencies of  $a_g(2)$ ,  $h_g(7)$ , and  $h_g(8)$  modes are close to each other.

Considering the ambiguity of the vibrational temperature in the experiment, these sets of VCCs cannot be distinguished. Thus, to obtain more accurate coupling constants, it is desired to perform an observation of a PES of  $C_{60}^-$  in still better experimental conditions. Although we find several sets of VCCs from the spectrum, the stabilization energies are similar to each other. In comparison with the total stabilization energy derived by Gunnarsson *et al.*,<sup>3</sup> our value is smaller by 30 %. We also calculated the VCCs using the DFT method. Even though the experimental and theoretical orders of  $E_{s,i}$  disagree with each other, the distribution of  $E_{JT,\mu}$  and the total stabilization energy  $E_s + E_{JT}$  agrees well with the experimental values. Thus we may conclude that the problem of the discrepancy between the experimental and calculated coupling constants, persistent in the previous studies, is basically solved in the present work. As an extension of the present work we expect that the theoretical approach used here could be successfully applied for the calculation of VCC of  $C_{60}^{n-}$  anions in  $A_nC_{60}$  fullerenes as well as of their multiplet splitting parameters.

### Appendix: Vibronic coupling constants and the gradient of Kohn–Sham levels

The total energy  $E(\mathbf{R})$  in the DFT is written as follows:

$$E(\mathbf{R}) = \sum_{\mu\Gamma\gamma} \epsilon_{\mu\Gamma\gamma}(\mathbf{R}) - \frac{1}{2} \int d\mathbf{r} \int d\mathbf{r}' \frac{n(\mathbf{r}; \mathbf{R})n(\mathbf{r}'; \mathbf{R})}{|\mathbf{r} - \mathbf{r}'|} + E_{xc}[n(\mathbf{r}; \mathbf{R})] - \int d\mathbf{r}n(\mathbf{r}; \mathbf{R})V_{xc}(\mathbf{r}; \mathbf{R}) + V_{nn}(\mathbf{R}). \quad (\text{A.1})$$

Here,  $\Gamma\gamma$  is the irreducible representation of the Kohn–Sham orbital,  $\mu$  is the quantum number other than  $\Gamma\gamma$ ,  $\epsilon_{\mu\Gamma\gamma}$  is the Kohn–Sham level,  $\sum_{\mu\Gamma\gamma}$  is taken over occupied levels,  $n(\mathbf{r}; \mathbf{R})$  is the ground electronic density,  $E_{xc}[n(\mathbf{r}; \mathbf{R})]$  is the exchange–correlation energy functional,  $V_{xc}(\mathbf{r}; \mathbf{R})$  is the exchange–correlation potential, and  $V_{nn}(\mathbf{R})$  is the Coulomb potential energy between nuclei. The vibronic coupling constant of  $\Gamma'\gamma'$  mode is

$$V_{\Gamma'\gamma'} = \sum_{\mu\Gamma\gamma} \left( \frac{\partial \epsilon_{\mu\Gamma\gamma}(\mathbf{R})}{\partial Q_{\Gamma'\gamma'}} \right)_{\mathbf{R}_0} - \int d\mathbf{r} \left( \frac{\partial n(\mathbf{r}; \mathbf{R})}{\partial Q_{\Gamma'\gamma'}} \right)_{\mathbf{R}_0} \int d\mathbf{r}' \frac{n(\mathbf{r}'; \mathbf{R})}{|\mathbf{r} - \mathbf{r}'|} - \int d\mathbf{r}n(\mathbf{r}; \mathbf{R}) \left( \frac{\partial V_{xc}(\mathbf{r}; \mathbf{R})}{\partial Q_{\Gamma'\gamma'}} \right)_{\mathbf{R}_0} + \left( \frac{\partial V_{nn}(\mathbf{R})}{\partial Q_{\Gamma'\gamma'}} \right)_{\mathbf{R}_0}. \quad (\text{A.2})$$

For the totally symmetric modes, all the derivatives in the right-hand side of Eq. (A.2) are not zero. For the Jahn–Teller active modes, the sum of the gradient of the completely occupied Kohn–Sham levels belonging to

the same  $\Gamma$  is zero due to the symmetry reasons, and the gradient of the Coulomb potential between the nuclei is zero also because of the symmetry. However, the second and third terms which include the derivative of

$n(\mathbf{r}; \mathbf{R})$  and  $V_{xc}(\mathbf{r}; \mathbf{R})$  with respect to  $Q_{\Gamma', \gamma'}$ , respectively, are nonzero because  $n(\mathbf{r}; \mathbf{R})$  is not a totally symmetric function. Therefore, in general, the vibronic coupling constant is not equal to the gradient of the frontier Kohn–Sham level.

## ACKNOWLEDGMENTS

We would like to thank Dr. X. B. Wang and Prof. L. S. Wang for sending us unpublished data. N.I. would like to thank the research fund for study abroad from the Research Project of Nano Frontier, graduate school of engineering, Kyoto University. T.S. and N.I. are grateful to

the Division of Quantum and Physical Chemistry at the University of Leuven for hospitality. Theoretical calculations were partly performed using Research Center for Computational Science, Okazaki, Japan. This work was supported by a Grant-in-Aid for Scientific Research, priority area Molecular theory for real systems (20038028) from the Japan Society for the Promotion of Science (JSPS). This work was also supported in part by the Global COE Program International Center for Integrated Research and Advanced Education in Materials Science (No. B-09) of the Ministry of Education, Culture, Sports, Science and Technology (MEXT) of Japan, administered by the JSPS. Financial support from the JSPS–FWO (Fonds voor Wetenschappelijk Onderzoek–Vlaanderen) bilateral program is gratefully acknowledged.

- 
- \* tsato@scl.kyoto-u.ac.jp  
 † Liviu.Chibotaru@chem.kuleuven.be
- <sup>1</sup> C. C. Chancey and M. C. M. O'Brien, *The Jahn–Teller Effect in C<sub>60</sub> and other Icosahedral Complexes* (Princeton University Press, Princeton, 1997).
  - <sup>2</sup> O. Gunnarsson, *Alkali-Doped Fullerenes: Narrow-Band Solids with Unusual Properties* (World Scientific, Singapore, 2004).
  - <sup>3</sup> O. Gunnarsson, H. Handschuh, P. S. Bechthold, B. Kessler, G. Ganteför, and W. Eberhardt, *Phys. Rev. Lett.*, **74**, 1875 (1995).
  - <sup>4</sup> J. Winter and H. Kuzmany, *Phys. Rev. B*, **53**, 655 (1996).
  - <sup>5</sup> I. D. Hands, J. L. Dunn, C. A. Bates, M. J. Hope, S. R. Meech, and D. L. Andrews, *Phys. Rev. B*, **77**, 115445 (2008).
  - <sup>6</sup> C. M. Varma, J. Zaanen, and K. Raghavachari, *Science*, **254**, 989 (1991).
  - <sup>7</sup> M. Schluter, M. Lannoo, M. Needels, G. A. Baraff, and D. Tománek, *Phys. Rev. Lett.*, **68**, 526 (1992).
  - <sup>8</sup> J. C. R. Faulhaber, D. Y. K. Ko, and P. R. Briddon, *Phys. Rev. B*, **48**, 661 (1993).
  - <sup>9</sup> V. P. Antropov, O. Gunnarsson, and A. I. Liechtenstein, *Phys. Rev. B*, **48**, 7651 (1993).
  - <sup>10</sup> N. Breda, R. A. Broglia, G. Colò, H. E. Roman, F. Alasia, G. Onida, V. Ponomarev, and E. Vigezzi, *Chem. Phys. Lett.*, **286**, 350 (1998).
  - <sup>11</sup> N. Manini, A. D. Carso, M. Fabrizio, and E. Tosatti, *Philos. Mag. B*, **81**, 793 (2001).
  - <sup>12</sup> M. Saito, *Phys. Rev. B*, **65**, 220508(R) (2002).
  - <sup>13</sup> T. Frederiksen, K. J. Franke, A. Arnau, G. Schulze, J. I. Pascual, and N. Lorente, *Phys. Rev. B*, **78**, 233401 (2008).
  - <sup>14</sup> J. Laflamme Janssen, M. Côté, S. G. Louie, and M. L. Cohen, *Phys. Rev. B*, **81**, 073106 (2010).
  - <sup>15</sup> X. B. Wang, H. K. Woo, and L. S. Wang, *J. Chem. Phys.*, **123**, 051106 (2005).
  - <sup>16</sup> M. C. M. O'Brien, *J. Phys. C: Solid St. Phys.*, **4**, 2524 (1971).
  - <sup>17</sup> A. Auerbach, N. Manini, and E. Tosatti, *Phys. Rev. B*, **49**, 12998 (1994).
  - <sup>18</sup> A. R. Edmonds, *Angular Momentum in Quantum Mechanics* (Princeton University Press, Princeton, 1974).
  - <sup>19</sup> M. C. M. O'Brien, *Phys. Rev.*, **187**, 407 (1969).
  - <sup>20</sup> I. B. Bersuker and V. Z. Polinger, *Vibronic Interactions in Molecules and Crystals* (Springer–Verlag, Berlin and Heidelberg, 1989).
  - <sup>21</sup> D. S. Bethune, G. Meijer, W. C. Tang, H. J. Rosen, W. G. Golden, H. Seki, C. A. Brown, and M. S. de Vries, *Chem. Phys. Lett.*, **179**, 181 (1991).
  - <sup>22</sup> L. Hedin and S. Lundqvist, in *Solid State Physics*, Vol. 23, edited by H. Ehrenreich, D. Turnbull, and F. Seitz (Academic Press, New York, 1969) p. 1.
  - <sup>23</sup> M. S. Child and H. G. Longuet-Higgins, *Phil. Trans. R. Soc. A*, **254**, 259 (1961).
  - <sup>24</sup> R. P. Feynman, *Phys. Rev.*, **56**, 340 (1939).
  - <sup>25</sup> A. D. Becke, *J. Chem. Phys.*, **98**, 5648 (1993).
  - <sup>26</sup> T. Sato, K. Tokunaga, and K. Tanaka, *J. Chem. Phys.*, **124**, 024314 (2006).
  - <sup>27</sup> T. Sato, K. Tokunaga, N. Iwahara, K. Shizu, and K. Tanaka, in *The Jahn–Teller Effect: Fundamentals and Implications for Physics and Chemistry*, edited by H. Köppel, D. R. Yarkony, and H. Barentzen (Springer–Verlag, Berlin and Heidelberg, 2009) p. 99.
  - <sup>28</sup> M. J. Frisch *et al.*, *Gaussian 03, Revision E.01*, Wallingford, CT (2004).
  - <sup>29</sup> B. Narymbetov, H. Kobayashi, M. Tokumoto, A. Omerzu, and D. Mihailovic, *Chem. Commun.*, 1511 (1999).
  - <sup>30</sup> M. Fujiwara, T. Kambe, and K. Oshima, *Phys. Rev. B*, **71**, 174424 (2005).
  - <sup>31</sup> W. I. F. David, R. M. Ibberson, J. C. Matthewman, K. Prassides, T. J. S. Dennis, J. P. Hare, H. W. Kroto, R. Taylor, and D. R. M. Walton, *Nature (London)*, **353**, 147 (1991).
  - <sup>32</sup> H. B. Bürgi, E. Blanc, D. Schwarzenbach, S. Z. Liu, Y. J. Lu, and M. Kappes, *Angew. Chem. Int. Ed. Engl.*, **31**, 640 (1992).
  - <sup>33</sup> Actually this line contains contributions also from temperature populated excited vibronic levels of C<sub>60</sub><sup>−</sup> to some excited vibrational levels of C<sub>60</sub>. However in the present case their contribution to the 0–0 line is very small.
  - <sup>34</sup> R. Bruyndonckx, C. Daul, P. T. Manoharan, and E. Deiss, *Inorg. Chem.*, **36**, 4251 (1997)